

Cell-based reporters reveal *in vivo* dynamics of dopamine and norepinephrine release in murine cortex

Arnaud Muller^{1,6}, Victory Joseph^{2,6}, Paul A Slesinger^{2,3} & David Kleinfeld^{1,2,4,5}

The neuronal coding of stimulus-to-action sequences is believed to involve the release of dopamine (DA) and norepinephrine (NE). The electrochemical similarity of these monoamines, however, confounds real-time measurements of their release. Here we report cell-based neurotransmitter fluorescent engineered reporters (CNiFERs) that use the specificity of G protein-coupled receptors (GPCRs) to discriminate nanomolar concentrations of DA and NE. CNiFERs were implanted into the frontal cortex of mice to measure the timing of neurotransmitter release during classical conditioning with the use of two-photon microscopy. The onset of DA release correlated with that of licking and shifted from the time of the reward toward that of the cue upon conditioning. In contrast, concurrent release of NE did not correlate with licking or the cue. This generation of CNiFERs provides unique tools to assess the release of monoamines. The molecular design of these CNiFERs may be generalized to realize CNiFERs for any molecule that activates a GPCR.

Neuronal processing in the cortex plays an essential role in the transformation of sensory perception into motor actions. Neurotransmitters, which signal via slow extrasynaptic pathways as well as fast synaptic pathways, are involved in the refinement of neuronal processing that underlies the execution of behaviors. Slow signaling occurs through volume transmission over a period of seconds^{1,2} and is believed to drive the plasticity of neural circuits and network activity. In particular, the monoamines DA and NE are required for the formation of working memories, changes in attention, enhancement of decision-making^{3–5} and perceptual learning^{6,7}. A major obstacle in neuroscience has been the inability to detect the release of DA and NE *in vivo* with sufficient chemical specificity, spatial resolution and temporal resolution.

Microdialysis is the most common technique to measure the extracellular concentration of neuromodulators *in vivo*⁸. Although microdialysis can accurately identify neurotransmitters^{9,10}, it requires the collection of relatively large samples and has poor temporal resolution, exceeding 10 min per sample in the case of monoamines¹¹. Moreover, the insertion of microdialysis probes can disrupt monoaminergic activity near the probe track¹².

The second method to measure the extracellular concentration of neuromodulators is fast-scan cyclic voltammetry (FSCV). This technique improves on the temporal and spatial resolution and has nanomolar sensitivity. The use of FSCV has been most successful for the detection of DA and serotonin, yet DA and NE, which differ by a single hydroxyl side group, have indistinguishable cyclic voltammetry signatures¹³. Thus, use of FSCV has been limited to areas of the brain in which either DA or NE, but not both, is thought to be present. For example, cyclic voltammetry is commonly used in the striatum, which receives a strong DA projection¹⁴. However, measuring DA and NE in the neocortex, which receives strong projections from dopaminergic and noradrenergic neurons, has remained a formidable challenge for cyclic voltammetry.

To address the current limitations in measuring neurotransmitters *in vivo*, we have developed a new technology to optically detect the release of neurotransmitters in the brain. Previously, we created a CNiFER for detecting acetylcholine¹⁵. CNiFERs are implanted into target brain regions, where they report changes in neurotransmitter release *in vivo*. Notable advantages of CNiFERs are their detection of nanomolar, physiological concentrations of neurotransmitter combined with their temporal resolution of seconds and spatial resolution of less than 100 μm .

CNiFERs are clonal cell lines engineered to express a specific GPCR that is coupled to the G_q pathway and triggers an increase in intracellular calcium concentration, $[\text{Ca}^{2+}]$, which in turn is rapidly detected by a genetically encoded fluorescence resonance energy transfer (FRET)-based Ca^{2+} sensor. This system transforms neurotransmitter receptor binding into a change in fluorescence and provides a direct and real-time optical readout of local neurotransmitter activity. Furthermore, by using the natural receptor for a given transmitter, CNiFERs gain the chemical specificity and temporal dynamics present *in vivo*.

Here we report the creation of two new CNiFERs to detect DA and NE. To test their function, we implanted these CNiFERs in the frontal cortex of mice and used *in vivo* two-photon imaging¹⁶ through a transcranial window¹⁷ to readdress the phenomenology of monoamine release during behavioral conditioning^{2,3,11,18–21}.

¹Department of Physics, University of California at San Diego, La Jolla, California, USA. ²Graduate Program in Neurosciences, University of California at San Diego, La Jolla, California, USA. ³Department of Neuroscience, Icahn School of Medicine at Mount Sinai, New York, New York, USA. ⁴Section of Neurobiology, University of California at San Diego, La Jolla, California, USA. ⁵Department of Electrical and Computer Engineering, University of California at San Diego, La Jolla, California, USA. ⁶These authors contributed equally to this work. Correspondence should be addressed to D.K. (dk@physics.ucsd.edu) or P.A.S. (paul.slesinger@mssm.edu).

RESULTS

Creation of CNiFERS to detect DA or NE

A CNiFER is derived from a HEK293 cell that stably expresses at least two proteins: a specific GPCR and TN-XXL, a genetically encoded FRET-based $[Ca^{2+}]$ sensor^{15,22}. Activation of GPCRs that couple to endogenous G_q proteins trigger an increase in cytosolic $[Ca^{2+}]$ through the phospholipase C–inositol triphosphate (PLC-IP₃) pathway, leading to an increase in FRET from the TN-XXL (Fig. 1a,b). This increase in FRET provides a rapid optical readout of the change in neurotransmitter levels. To develop CNiFERS for detecting DA and for NE, we selected two GPCRs with high affinity and selectivity: the D2 dopaminergic receptor and the α_{1A} adrenergic receptor (Fig. 1a,b). The α_{1A} adrenergic receptor couples to G_q proteins and could be introduced directly into HEK293 cells. The D2 dopaminergic receptor couples to G_i and G_o ($G_{i/o}$) proteins and first required the creation of a clonal HEK293 line that expresses G_{qi5} , a chimeric G protein²³. This chimeric G protein contains primarily the $G\alpha_q$ sequence for signaling through the PLC-IP₃ pathway, but the five amino acids of the carboxyl terminus have been replaced with those of $G\alpha_{i/o}$ to enable coupling to the D2 receptor (Fig. 1a,b).

To identify the CNiFER clones with the best sensitivity to the native ligand and smallest response to other neurotransmitters, we used a high-throughput fluorometric plate reader to screen the individual clonal lines. Two lines, D2 CNiFER (clone D2.2) and α_{1A} CNiFER (clone $\alpha_{1A}.6$), were selected for more detailed analyses. The parent lines lacking the receptors (clones 3g8 and qi5.6) served as control CNiFERS. An example of the FRET response from the plate reader shows that agonist application led to a step-decrease of enhanced CFP (ECFP; FRET donor) emission and a step-increase of Citrine (FRET acceptor) emission (Fig. 1c). The calculated fractional change in fluorescence, $\Delta F/F$, for each signal was used to obtain the FRET ratio, denoted $\Delta R/R$ (Fig. 1c).

In vitro characterization of D2 and α_{1A} CNiFERS

How sensitive and specific are the new CNiFERS to the chosen agonists? The D2 CNiFER displayed nanomolar sensitivity to DA, with an effector concentration for half-maximum response (EC_{50}) of 2.5 ± 0.1 nM (mean \pm s.e.m. throughout unless otherwise specified; $n = 3$ runs), and a response to NE that was ~ 30 times less sensitive than the response to DA ($EC_{50} = 81 \pm 8$ nM for NE). Similarly, the α_{1A} CNiFER exhibited nanomolar sensitivity to NE with an $EC_{50} = 19 \pm 1$ nM ($n = 3$) and a DA response only

at high concentrations ($EC_{50} = 1.4 \pm 0.1$ μ M for DA) (Fig. 1d). Notably, the dynamic ranges of the D2 and α_{1A} CNiFERS were comparable to the levels of monoamines measured with microdialysis^{11,24,25} and FSCV^{26,27} in the rodent brain. As a control, we examined HEK293 lines lacking the GPCR. We observed that the G_{qi5} -TN-XXL HEK293 line qi5.6 and TN-XXL HEK293 line 3g8 showed an insignificant FRET response to either DA or NE at high concentrations ($n = 3$ for each condition, $P > 0.08$; Fig. 1d).

To screen for nonspecific receptor activation, we tested a set of common neurotransmitters at a low (50 nM) and high (1 μ M) concentration (Fig. 1e). The D2 CNiFER did not show appreciable response to most agonists and responded only weakly to somatostatin ($\Delta R/R = 0.2$), acetylcholine ($\Delta R/R = 0.1$) and vasointestinal peptide ($\Delta R/R = 0.1$) at 1 μ M. The α_{1A} CNiFER showed negligible responses to the tested agonists.

As HEK293 cells possess endogenous GPCRs, we investigated the pharmacological receptor specificity of the D2 and α_{1A} CNiFERS (Supplementary Fig. 1). The D2-CNiFER response to 20 nM DA was not significantly altered following preincubation with the D1-receptor antagonist SCH23390 (100 nM) (normalized $\Delta R/R = 1.00 \pm 0.03$, $n = 5$, $P = 0.99$, unpaired *t*-test) but

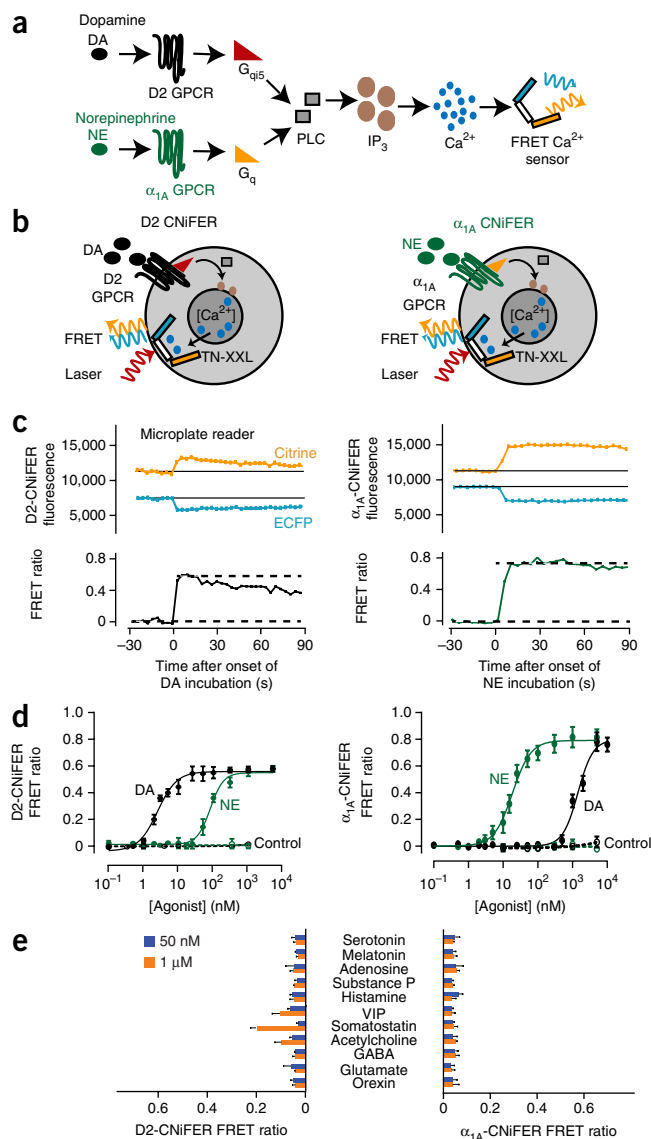


Figure 1 | Design of D2 and α_{1A} CNiFERS and their *in vitro* characterization using a high-throughput plate reader. **(a)** Schematic of the CNiFER signaling pathways. **(b)** Depiction of DA activating the D2 receptor (left, black) and NE activating the α_{1A} receptor (right, green) to induce Ca^{2+} cytoplasmic influx detected by TN-XXL. Fluorescence from laser-excited ECFP and Citrine flanking TN-XXL is collected for the FRET signal. **(c)** FRET response of D2 CNiFER to continuous application of 100 nM DA (left) and α_{1A} CNiFER to continuous application of 100 nM NE (right). An example of transmitter-induced responses in orange (530 nm) and cyan (475 nm) fluorescence ($\Delta F/F$; top) represented as a FRET ratio ($\Delta R/R$; bottom) is shown. **(d)** Left, dose-response curves for D2 CNiFER and control CNiFERS (calcium indicator and chimeric G_{qi5} protein only) in response to DA or NE ($n = 3$). Right, dose-response curves for α_{1A} CNiFER and control CNiFERS (calcium indicator only) in response to DA or NE ($n = 3$). Error bars, s.d. **(e)** Summary of D2-CNiFER and α_{1A} -CNiFER FRET responses to a panel of neurotransmitters at 50 nM and 1 μ M. VIP, vasoactive intestinal peptide; GABA, γ -aminobutyric acid. Error bars, s.d. ($n = 3$).

Figure 2 | *In vitro* characterization of CNiFER response to agonist pulses. (a) Single-trial FRET response of a cluster of ~50 D2 CNiFERs to a 2.5-s pulse of 100 nM DA (left) and of a cluster of approximately 50 α_{1A} CNiFERs to a 2.5-s pulse of 100 nM NE (right). Top, examples of transmitter-induced FRET responses for D2 CNiFER and α_{1A} CNiFER. Bottom, FRET ratio ($\Delta R/R$). 'Dye', Alexa Fluor 594 fluorescence to monitor the time course of the agonist pulse. (b) Left, temporal discrimination of D2-CNiFER FRET responses to delivery of two 2.5-s pulses of 100 nM DA with variable interstimulus intervals ($n = 3$). Right, discrimination of α_{1A} -CNiFER responses to two pulses of 100 nM NE ($n = 3$). Shaded areas represent standard error. (c) D2-CNiFER and α_{1A} -CNiFER FRET responses to repeated 60-s pulses of 50 nM DA (black dashes; $n = 3$) or 500 nM NE (green dashes; $n = 3$) followed by 180 s of artificial cerebral spinal fluid. Shaded areas are standard error.

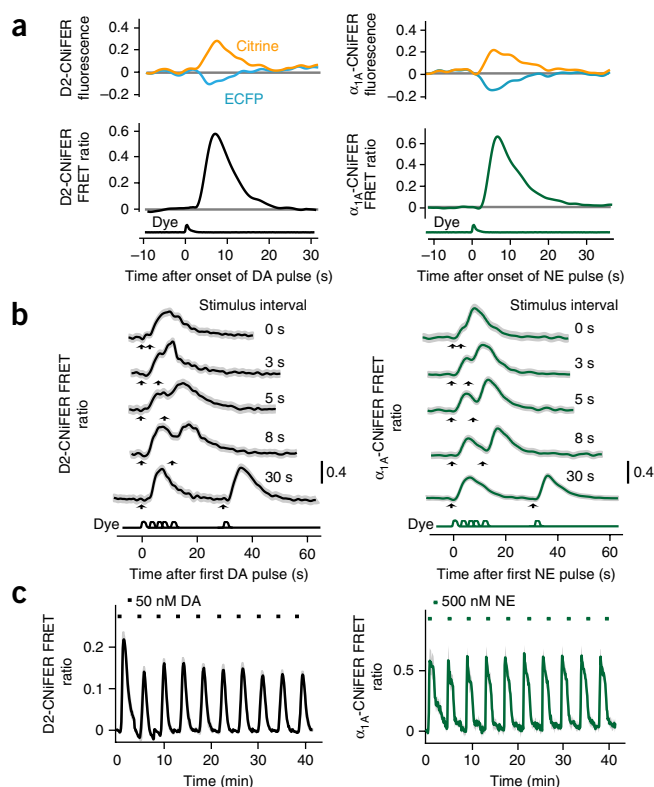
was fully blocked by preincubation with the D2-receptor antagonist eticlopride (50 nM) (normalized $\Delta R/R = 0.04 \pm 0.02$, $n = 5$, $P = 0.0003$, unpaired t -test). Similarly, the α_{1A} -CNiFER response to 50 nM NE was not significantly altered by preincubation with the β -adrenergic-receptor antagonist sotalol (5 μ M) (normalized $\Delta R/R = 0.82 \pm 0.10$, $n = 4$, $P = 0.17$, unpaired t -test) but was strongly suppressed by preincubation with the α_{1A} -antagonist WB4101 (50 nM) (normalized $\Delta R/R = 0.09 \pm 0.03$, $n = 4$, $P = 0.0001$, unpaired t -test). Taken together, these data establish the specificity of the D2 and α_{1A} CNiFERs.

The natural release of both NE and DA *in vivo* can be pulsatile. To determine the response of CNiFERs to a pulse of agonist, we used a fast perfusion system to apply pulses at near-saturating concentrations to a cluster of CNiFERs, i.e., 2.5-s pulses of 100 nM agonist mixed with a fluorescent dye (Fig. 2a). At the level of individual cells ($n = 20$), a D2 CNiFER responded with a delay of 2.9 ± 0.2 s, reached a maximum response at 6.9 ± 0.6 s after the pulse onset and had a maximum FRET ratio of 0.57 ± 0.03 (± 0.13 s.d. for a cell-to-cell variability of 23%) (Supplementary Fig. 2a). Similarly, pulses of NE increased the FRET ratio for an individual α_{1A} CNiFER with a delay of 2.3 ± 0.1 s, reached a maximum at 5.1 ± 0.3 s and had a FRET ratio of 0.90 ± 0.05 (± 0.22 s.d. for a cell-to-cell variability of 24%) (Supplementary Fig. 2b). At this agonist concentration, the FRET signal returned to baseline in ~20 s. This recovery time can likely be accounted for by the intrinsic properties of the GPCR signaling pathway^{28,29}. Our data show that individual CNiFERs exhibit a reliable, robust response to pulsatile changes in agonist concentration.

To determine how CNiFERs respond to repeated agonist stimulation and to assess the temporal resolution of the new CNiFERs, we used two 2.5-s pulses of agonist that were separated by a variable amount of time (Fig. 2b). The FRET responses of both D2 and α_{1A} CNiFERs could be distinguished with an interstimulus interval of only 5 s. We also investigated possible receptor desensitization using a 5-s pulse delivered every 4 min for 40 min (Fig. 2c). The D2-CNiFER response decreased slightly between the first and the second pulse of agonist but remained stable thereafter ($n = 3$) (Fig. 2c). The α_{1A} CNiFER showed a consistent FRET ratio across pulses ($n = 3$) (Fig. 2c). Taken together, these experiments demonstrate that both the D2 and α_{1A} CNiFERs respond reliably with little attenuation to repeated neurotransmitter exposure.

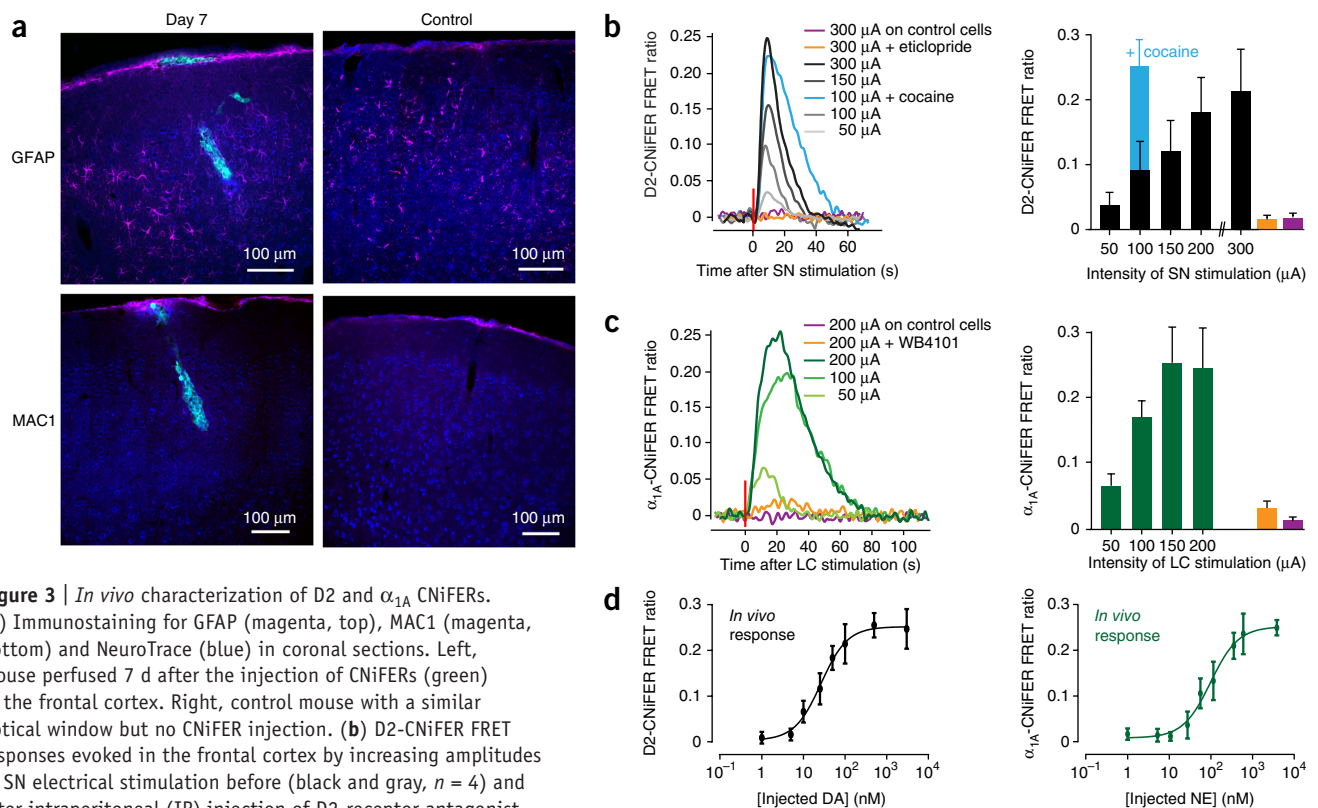
***In vivo* characterization of D2 and α_{1A} CNiFERs**

We first established that each CNiFER could detect endogenous release of neurotransmitters. The mesolimbic DA circuit involves



two primary DA pathways: (i) ventral tegmental area DA neurons that project to the ventral striatum (nucleus accumbens) and medial prefrontal cortex and (ii) substantia nigra (SN) DA neurons that project to the dorsal striatum and broadly to cortical regions³⁰. To confirm the presence of direct projections from both dopaminergic and noradrenergic nuclei to the frontal cortex, we injected a neuronal retrograde tracer, Fluorogold, in the frontal cortex and searched for neurons colabeled with Fluorogold and tyrosine hydroxylase, a biosynthetic enzyme for both DA and NE (Supplementary Fig. 3a,b). Three-dimensional reconstructions revealed that the majority of dopaminergic projections to the frontal cortex originated from the SN ($95\% \pm 2\%$ of colabeled neurons, $n = 4$) (Supplementary Fig. 3c), confirming results from previous studies^{30–32}. We observed few neurons colabeled for Fluorogold and tyrosine hydroxylase in the mouse ventral tegmental area ($5\% \pm 2\%$ of colabeled neurons), although such projections to the frontal cortex have been reported³³. Three-dimensional reconstruction also revealed that the noradrenergic inputs originated from the locus coeruleus (LC) (Supplementary Fig. 3c), corroborating previous studies^{34,35}.

An advantage of implanting CNiFERs in the brain is that repeated measurements can be made across multiple days of behavioral training and experimentation. We stereotactically injected CNiFERs into mouse frontal cortex at discrete sites located 200–300 μ m below the cortical surface, i.e., layer 2/3 (Fig. 3a). To address the possibility that the required surgical procedure or presence of human cells introduced damage or inflammation in the cortex, we prepared mice for histological assessment of inflammation 7 d after implantation of the CNiFERs. Immunostaining for glial fibrillary acidic protein (GFAP), a marker of inflammation, revealed a small increase in GFAP-positive cells in both injected and control mice (Fig. 3a). This indicates that the presence of



CNiFER cells did not induce substantial damage even though the surgical procedure led to inflammation. Critically, no glial scars were found around the CNiFERS 1 week after the implantation. To examine activated microglia, we performed immunostaining for MAC1 and did not observe any detectable staining, which is consistent with claims that a thinned skull preparation does not induce an apparent inflammatory response¹⁷. Taken together, these experiments suggest there is minimal damage caused by the injection of HEK293 cells into the cortex of mice.

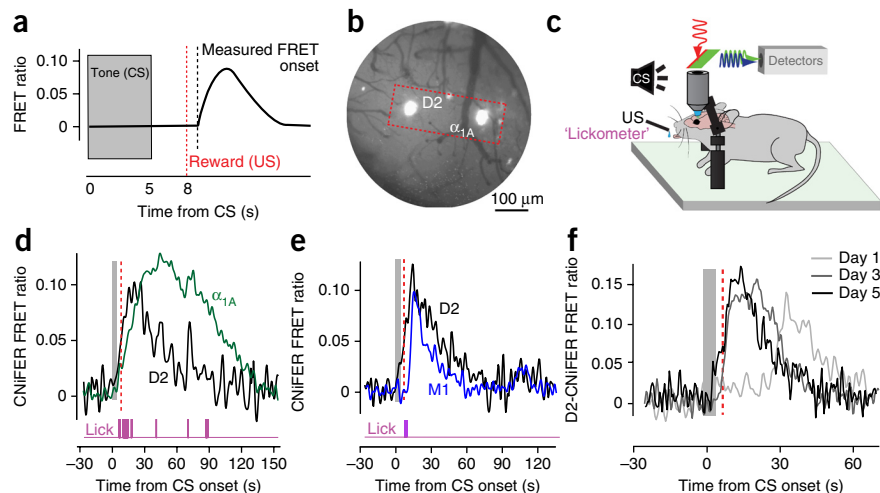
We examined whether the D2 and α_{1A} CNiFERS could detect an induced release of DA or NE, respectively, in the chronic preparation. We stereotaxically implanted electrodes into either the SN or LC for electrical stimulation and stereotaxically injected CNiFERS into the frontal cortex. Each *in vivo* two-photon imaging plane contained 5–20 CNiFERS. After 1 d of recovery, a single burst of electrical stimulation in the SN led to an increase in the FRET ratio for the D2 CNiFER within 2 s of the stimulation. The amplitude of the FRET response varied with the amplitude of the stimulation, with 100- μ A stimulation producing a $\Delta R/R = 0.09 \pm 0.02$ ($n = 4$) (Fig. 3b). We next measured the effect of cocaine on the D2-CNiFER response upon electrical stimulation of the SN. As expected for a DA reuptake inhibitor, 15 mg cocaine per kilogram body weight (mg/kg; intraperitoneal injection) enhanced the size of the D2-CNiFER FRET response, with a 100- μ A stimulation now producing a $\Delta R/R = 0.24 \pm 0.02$ ($P < 0.01$, unpaired *t*-test, $n = 3$) (Fig. 3b). The duration of the signal, measured from the

onset of the response to the return to the baseline, also increased from 27 ± 4 s to 61 ± 7 s after the cocaine injection.

Like the response of D2 CNiFERS to SN stimulation, the α_{1A} -CNiFER response increased following electrical stimulation of the LC (Fig. 3c; $n = 3$), with a $\Delta R/R = 0.17 \pm 0.02$ for a 100- μ A stimulation. Thus, both D2 and α_{1A} CNiFERS exhibited a dynamic range *in vivo* suitable to measure release of DA and NE in behaving mice. We confirmed the receptor specificity of each CNiFER *in vivo* with systemic injection of receptor-specific antagonists that blocked CNiFER responses to electrical stimulation (Fig. 3b,c) ($P = 0.0004$ for eticlopride versus normal response to SN stimulation for D2 CNiFERS; $P = 0.004$ for WB4101 versus normal response to LC stimulation for α_{1A} CNiFERS; unpaired *t*-test, $n = 3$ for both). In addition, control CNiFERS showed little response to electrical stimulation (Fig. 3b,c) ($P = 0.0005$ for control cells versus D2 CNiFERS in response to SN stimulation and $P = 0.003$ for control cells versus α_{1A} CNiFERS in response to LC stimulation, unpaired *t*-test, $n = 3$ for both). The duration of the FRET response varied from 20 s with weak stimulation to more than 1 min with strong stimulation (Fig. 3b,c), consistent with CNiFERS detecting volume transmission of neurotransmitters in the cortex.

We determined whether D2 and α_{1A} CNiFERS maintain their sensitivity *in vivo*. CNiFERS were stereotaxically injected into the frontal cortex, and a micropipette was placed with a tip approximately 100 μ m from the implant. We measured the *in vivo* response of a cluster of CNiFERS to a train of pulses of

Figure 4 | Simultaneous detection of DA, NE and ACh release during behavioral conditioning. (a) Schematic of CNiFER FRET response and onset measurement during a single conditioning trial. Conditioning trials consisted of a 5-s tone (conditioning stimulus, CS) followed by a 3-s delay and delivery of a drop of 10% (w/v) sucrose water (unconditioned stimulus, US). (b) Bright-field image of the surface vasculature superimposed with fluorescent picture of the CNiFERs. D2 CNiFERs and α_{1A} CNiFERs were implanted next to each other in the frontal cortex. The red box shows the field of view that was used to image both CNiFERs simultaneously. (c) Procedure to measure licking behavior and CNiFER fluorescence in head-restrained mice during classical conditioning. (d) Simultaneous measurement of D2- and α_{1A} -CNiFER FRET responses and licking during a single conditioning trial. (e) Simultaneous measurement of D2- and M1-CNiFER FRET responses and licking during a single conditioning trial. (f) Single trace examples of the D2-CNiFER response in the same animal at days 1, 3 and 5 of training.



agonist delivered concurrently with a fluorescent indicator. The D2 CNiFER displayed an *in vivo* sensitivity to DA with an $EC_{50} = 29 \pm 5$ nM ($n = 4$), whereas the α_{1A} CNiFER exhibited an *in vivo* sensitivity to NE with an $EC_{50} = 90 \pm 21$ nM ($n = 4$) (Fig. 3d). An increase in the apparent *in vivo* values for EC_{50} compared with the *in vitro* values was expected from the dilution of agonist as it diffused from the pipette to the site of the implant³⁶. The observed dilution of 0.16 ± 0.03 ($n = 14$) explains half of the apparent increase in EC_{50} for D2 CNiFERs and all of the increase for α_{1A} CNiFERs compared to the *in vitro* results (Fig. 1d). The remaining difference could result from *in situ* effects of the brain environment on the sensitivity of the D2 GPCR.

Simultaneous measurement of neuromodulators during learning

Classically conditioned cue-reward pairings increase neuronal firing in midbrain neurons, with a temporal shift from the time of the reward, i.e., the unconditioned stimulus (US), to the time of the predictive cue, i.e., the conditioned stimulus (CS). Similarly, neurons in the LC transiently spike in response to task-relevant stimuli^{3,21}, suggesting that NE levels may also increase in the cortex during conditioning. Using the D2 and α_{1A} CNiFERs, we probed the timing of DA and NE release during learning using a basic Pavlovian conditioning paradigm in head-fixed mice (Fig. 4).

We implemented a paradigm consisting of a 5-s tone (CS) followed by a drop of 10% sucrose solution (US) that was delivered 3 s after the end of the tone (Fig. 4a). Prior to training the mice, we injected them with only D2 CNiFERs, or with D2 and α_{1A} CNiFERs in discrete sites separated by ~ 300 μ m, in layers 2/3 of the frontal cortex (Fig. 4b). We then simultaneously measured FRET responses from the CNiFERs and licking behavior while mice learned to associate the tone with delivery of the sucrose solution (Fig. 4c). Although the delivery of the reward was not dependent on the animal's behavior, sucrose retrieval required the motor act of tongue protrusion and licking. We hypothesized that the release of DA in the frontal cortex would shift from the time of the reward to the time of the predictive cue (CS). In an additional cohort of mice, we implanted M1 CNiFERs¹⁵, which express a muscarinic receptor, and the D2 CNiFERs in two distinct

locations in the same brain area. We predicted engagement of the cholinergic (ACh) system in the frontal cortex when animals made an explicit movement³⁷ such as licking.

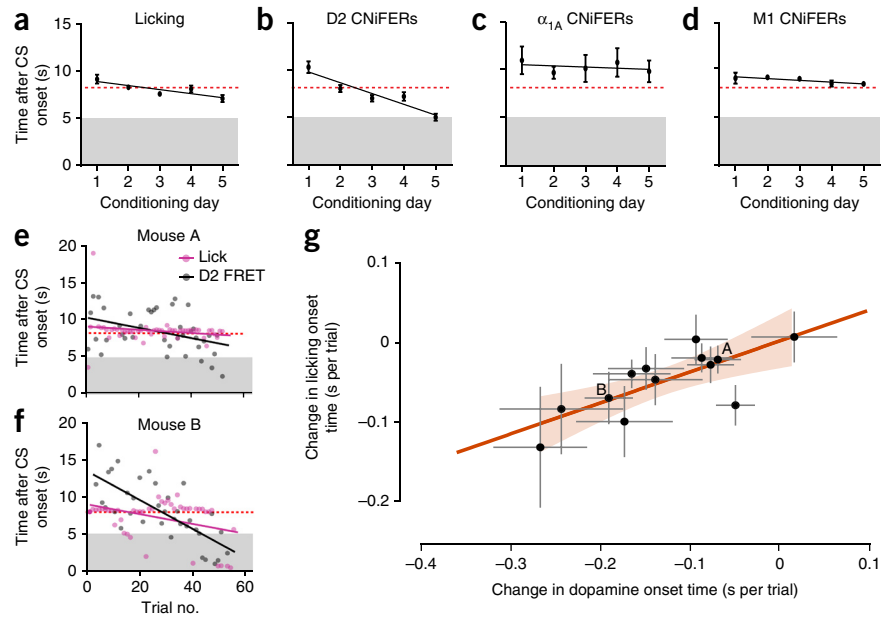
We detected an increase in the FRET ratio for both D2 and α_{1A} CNiFERs within a single trial of conditioning and with a high signal-to-noise ratio (Fig. 4d). Simultaneous measurements of the D2- and M1-CNiFER responses, and concomitant licking, were also observed on a single-trial basis with a high signal-to-noise ratio during conditioning trials (Fig. 4e). The transient increases in DA and NE were similar in duration, with a full-width at half-maximum amplitude of 25 ± 1 s (13 mice) and 28 ± 1 s (8 mice) for DA and NE, respectively. In contrast, ACh transients in response to a burst of licks persisted for a shorter interval, i.e., 15 ± 1 s (4 mice).

The onset time of licking across multiple days of training exhibited a monotonic shift from the time of the reward to that of the cue. We observed a statistically significant decrease in the time to lick, with a slope of -0.40 ± 0.14 s per day ($P = 0.05$, linear regression; 13 mice) (Fig. 5a and Supplementary Fig. 4a). These data confirmed that mice learned to associate the CS with the US.

Do changes in volume transmission of DA and NE track the change in licking behavior? We observed a statistically significant decrease in the onset time of the FRET ratio with the D2 CNiFER across multiple days of training (Fig. 4f). As a population response, we observed a shift in the mean onset time of licking from 10.3 ± 0.6 s (13 mice) during the first day of training to 5 ± 0.3 s during the last day of training, with a slope of -1.1 ± 0.14 s per day ($P = 0.02$; 13 mice) (Fig. 5b and Supplementary Fig. 4b). Thus the release of DA shifted monotonically from the time of the reward toward the time of the cue, similarly to licking. In contrast, the onset of the α_{1A} -CNiFER FRET response did not show an appreciable change across conditioning days, with an average delay of 10.8 ± 1.4 s during the first day of training and 9.7 ± 1.1 s during the last day of training ($P = 0.6$; 7 mice) (Fig. 5c and Supplementary Fig. 4c). Notably, the timing of NE release was highly variable both within a set of trials for a given animal and across animals over conditioning days.

The release of ACh, unlike that of DA, remained closely linked to the time of presentation of the reward across conditioning trials. The M1-CNiFER FRET onset shifted from 9.0 ± 0.6 s (4 mice)

Figure 5 | Shift in DA but not NE release with behavioral conditioning. (a–d) Population averages of response onsets. (a) Licking onsets ($n = 13$) on days 1–5 of conditioning. Error bars, standard error. Gray, CS; dashed red line, US. (b–d) D2-CNiFER FRET-response onsets ($n = 13$) (b), α_{1A} -CNiFER FRET-response onsets ($n = 7$) (c) and M1-CNiFER FRET-response onsets (d) during conditioning, shown relative to CS onset. (e,f) Onset of D2-CNiFER FRET response and licking across conditioning trials for two mice (A and B). Solid lines, best-fit linear regressions of CNiFER responses and licking; gray, time of CS presentation; dashed red line, time of US presentation. (g) Correlation between rate of change in DA onset and rate of change in licking onset across conditioning trials. Each point represents the rate relationship for one animal with s.d. (gray error bars). Orange line, linear regression with 95% confidence intervals (orange shaded area, $n = 13$).



during the first day of training to 8.4 ± 0.3 s during the last day of training, with a slope of -0.2 ± 0.05 s per day ($P = 0.04$) (Fig. 5d and Supplementary Fig. 4d). The onset always occurred after the presentation of the reward at 8.0 s. In the absence of any reward, we observed a transient release of ACh when animals engaged in bouts of high-frequency licking, similar to reward retrieval (15 events across 4 mice) (Supplementary Fig. 4e). These findings suggest that ACh release may be involved in the motor behavior of licking following presentation of the reward (US). However, ACh release could not be detected by the M1 CNiFERs during anticipatory licking, in contrast to DA release.

Correlation of DA release with anticipatory licking

Real-time measurements of neurotransmitter release revealed that the release of DA correlated with learning the association of CS with US, whereas the release of NE appeared uncorrelated. We next examined the shift in timing of DA release on a trial-by-trial basis for each mouse. Mice that exhibited a small change in the timing of DA release did not show significant anticipatory licking (Fig. 5e). By contrast, mice that demonstrated a strong shift in DA release also demonstrated a significant change in anticipatory licking (Fig. 5f). For all 13 mice, we compared the rates of change in DA release and in anticipatory licking across all trials and found that they were strongly and significantly correlated (slope = 0.4 ± 0.1 , $P = 0.003$) (Fig. 5g). There was no significant correlation between the highly variable release of NE (Fig. 5c) and the animal's licking behavior ($P = 0.10$). We conclude that DA release tracks the extent of learning as defined by changes in the licking behavior.

DISCUSSION

Here we report the creation of a new family of cell-based CNiFERs for rapid, optical detection of monoamine neurotransmitters released *in vivo*. Previously, CNiFERs were limited to GPCRs that coupled to G_q proteins¹⁵. Yet redirecting the $G_{i/o}$ -coupled D2 receptor to the PLC-IP₃ pathway should now make it possible to create CNiFERs for other $G_{i/o}$ -coupled receptors, such as those for somatostatin, serotonin and opioids. With their nanomolar

sensitivity, temporal resolution of seconds and wide dynamic range, these CNiFERs offer significant advantages over current methods for detecting neurotransmitter release *in vivo*^{12,13}. The D2 and α_{1A} CNiFERs can provide real-time optical measurements of both DA and NE release *in vivo* with relatively little impact on the brain.

The method described here to detect changes in the FRET ratio from multiple CNiFERs is ideal for imaging experiments with head-fixed mice. Implanting CNiFERs into subcortical structures and using a fiber^{38,39} or gradient index lens/endoscope^{40,41} to measure changes in FRET could be used to study neuromodulation in freely moving animals. Creating CNiFERs with different sensitivities could provide new information about the status of signaling through various second-messenger pathways. For example, a DA-sensitive CNiFER for detecting higher concentrations of DA could be developed with the D1 receptor, which signals via the G_s pathway⁴². The methodology developed here to detect DA and NE could also be expanded to any neurotransmitter that signals through a GPCR and thus provides an important and versatile tool for neuroscientists that study circuit dynamics and brain states. Although the CNiFERs may well be supplanted by the development of molecular indicators that are expressed on the surface of neurons or glia, such technologies are currently available only for the detection of glutamate^{43,44} and are 100-fold less sensitive than CNiFERs. Moreover, these molecular detectors may also alter the physiology of the neuron or glial cell.

The ability of the D2 CNiFER and α_{1A} CNiFER to chemically discriminate NE from DA at fast temporal resolution provides a unique opportunity to analyze the dynamics of neurotransmitter release on a trial-by-trial basis during learning. Our results are consistent with those of previous studies that demonstrate that firing rates of DA neurons in the basal ganglia increase in response to rewarding stimuli^{45–48}. Our findings also agree with the proposed temporal difference model^{20,49}, in which DA neurons respond to reward-predicting cues. However, they contrast with a previous study of midbrain DA neurons in which these neurons increased their firing rate either just after the reward or just after the cue⁵⁰. Similarly, studies using FSCV demonstrated

a shift in DA release from the US to CS in the nucleus accumbens of rats^{26,27}. One possible difference is that the 5-s period of the CS used in our study might have facilitated the observation of a more gradual shift of the response to the start of the cue. Alternatively, the firing of DA neurons in the midbrain may not correlate with release of DA in the cortex, though this scenario seems unlikely. Optogenetic control of DA neuronal activity showed that phasic firing enhances DA release in the striatum², though DA levels were not measured in the cortex.

Whereas DA release appeared tightly correlated with the CS, NE release was highly variable. Other groups have shown that, similarly to DA neurons, LC neurons fire in tonic and burst modes, with LC phasic firing typically occurring following task cues (CS) but preceding lever responses (US)^{3,4,21}. ACh release, on the other hand, correlated with the US and licking but not with the CS. Thus, ACh and NE are both released during training trials but appear to respond to different cues. In conclusion, with the development of these new D2 and α_{1A} CNiFERS, along with the M1 CNiFER¹⁵, it will be now possible to study the spatial and temporal resolution of multiple neurotransmitters released in more complex behavioral tasks.

METHODS

Methods and any associated references are available in the [online version of the paper](#).

Note: Any Supplementary Information and Source Data files are available in the online version of the paper.

ACKNOWLEDGMENTS

We thank B. Conklin (University of California, San Francisco) for providing the G_{q15} cDNA, A. Schweitzer for assistance with the electronics, N. Taylor for assistance with screening of clones, and T. Komiyama and W. Schultz for discussions. This work was supported by research grants through the US National Institute on Drug Abuse (NIDA) (DA029706), the National Institute of Biomedical Imaging and Bioengineering (NIBIB) (EB003832), Hoffman-La Roche (88610A) and the “Neuroscience Related to Drugs of Abuse” training grant through NIDA (DA007315).

AUTHOR CONTRIBUTIONS

All authors contributed to the experimental design and realization, analysis of the data and writing of the paper. A.M. and V.J. performed the *in vitro* testing and *in vivo* imaging and behavioral experiments. D.K. and P.A.S. dealt with the myriad of university organizations that govern animal health and welfare, surgical procedures, and laboratory health and safety issues that include specific oversight of chemicals, controlled substances, human cell lines, lasers and viruses.

COMPETING FINANCIAL INTERESTS

The authors declare no competing financial interests.

Reprints and permissions information is available online at <http://www.nature.com/reprints/index.html>.

- Adamantidis, A.R. *et al.* Optogenetic interrogation of dopaminergic modulation of the multiple phases of reward-seeking behavior. *J. Neurosci.* **31**, 10829–10835 (2011).
- Tsai, H.C. *et al.* Phasic firing in dopaminergic neurons is sufficient for behavioral conditioning. *Science* **324**, 1080–1084 (2009).
- Aston-Jones, G. & Cohen, J.D. Adaptive gain and the role of the locus coeruleus-norepinephrine system in optimal performance. *J. Comp. Neurol.* **493**, 99–110 (2005).
- Bouret, S. & Sara, S.J. Network reset: a simplified overarching theory of locus coeruleus noradrenergic function. *Trends Neurosci.* **28**, 574–582 (2005).
- Floresco, S.B. Prefrontal dopamine and behavioral flexibility: shifting from an “inverted-U” toward a family of functions. *Front. Neurosci.* **7**, 62 (2013).
- Edeline, J.M., Manunta, Y. & Hennevin, E. Induction of selective plasticity in the frequency tuning of auditory cortex and auditory thalamus neurons by locus coeruleus stimulation. *Hear. Res.* **274**, 75–84 (2011).
- Bao, S., Chan, V.T. & Merzenich, M.M. Cortical remodelling induced by activity of ventral tegmental dopamine neurons. *Nature* **412**, 79–83 (2001).
- Day, J.C., Kornecook, T.J. & Quirion, R. Application of *in vivo* microdialysis to the study of cholinergic systems. *Methods* **23**, 21–39 (2001).
- Greco, S., Danysz, W., Zivkovic, A., Gross, R. & Stark, H. Microdialysate analysis of monoamine neurotransmitters—a versatile and sensitive LC-MS/MS method. *Anal. Chim. Acta* **771**, 65–72 (2013).
- Ji, C. *et al.* Diethylation labeling combined with UPLC/MS/MS for simultaneous determination of a panel of monoamine neurotransmitters in rat prefrontal cortex microdialysates. *Anal. Chem.* **80**, 9195–9203 (2008).
- Mingote, S., de Bruin, J.P.C. & Feenstra, M.G. Noradrenergic and dopamine efflux in the prefrontal cortex in relation to appetitive classical conditioning. *J. Neurosci.* **24**, 2475–2480 (2004).
- Wang, Y. & Michael, A.C. Microdialysis probes alter presynaptic regulation of dopamine terminals in rat striatum. *J. Neurosci. Methods* **208**, 34–39 (2012).
- Robinson, D.L., Venton, B.J., Heien, M.L. & Wightman, R.M. Detecting subsecond dopamine release with fast-scan cyclic voltammetry *in vivo*. *Clin. Chem.* **49**, 1763–1773 (2003).
- Park, J., Takmakov, P. & Wightman, R.M. *In vivo* comparison of norepinephrine and dopamine release in rat brain by simultaneous measurements with fast-scan cyclic voltammetry. *J. Neurochem.* **119**, 932–944 (2011).
- Nguyen, Q.-T. *et al.* An *in vivo* biosensor for neurotransmitter release and *in situ* receptor activity. *Nat. Neurosci.* **13**, 127–132 (2010).
- Svoboda, K., Denk, W., Kleinfeld, D. & Tank, D.W. *In vivo* dendritic calcium dynamics in neocortical pyramidal neurons. *Nature* **385**, 161–165 (1997).
- Drew, P.J. *et al.* Chronic optical access through a polished and reinforced thinned skull. *Nat. Methods* **7**, 981–984 (2010).
- Schultz, W. Updating dopamine reward signals. *Curr. Opin. Neurobiol.* **23**, 229–238 (2013).
- Feenstra, M.G. Dopamine and noradrenaline release in the prefrontal cortex in relation to unconditioned and conditioned stress and reward. *Prog. Brain Res.* **126**, 133–163 (2000).
- Schultz, W., Dayan, P. & Montague, P.R. A neural substrate of prediction and reward. *Science* **275**, 1593–1599 (1997).
- Bouret, S. & Richmond, B.J. Relation of locus coeruleus neurons in monkeys to Pavlovian and operant behaviors. *J. Neurophysiol.* **101**, 898–911 (2009).
- Yamauchi, J.G. *et al.* Characterizing ligand-gated ion channel receptors with genetically encoded Ca^{2+} sensors. *PLoS ONE* **6**, e16519 (2011).
- Conklin, B.R., Farfel, Z., Lustig, K.D., Julius, D. & Bourne, H.R. Substitution of three amino acids switches receptor specificity of $G_{q\alpha}$ (to that of G_{α}). *Nature* **363**, 274–276 (1993).
- Engleman, E.A., Ingraham, C.M., McBride, W.J., Lumeng, L. & Murphy, J.M. Extracellular dopamine levels are lower in the medial prefrontal cortex of alcohol-preferring rats compared to Wistar rats. *Alcohol* **38**, 5–12 (2006).
- Ihalainen, J.A., Riekkinen, P. Jr. & Feenstra, G.P. Comparison of dopamine and noradrenaline release in mouse prefrontal cortex, striatum and hippocampus using microdialysis. *Neurosci. Lett.* **277**, 71–74 (1999).
- Clark, J.J. *et al.* Chronic microsensors for longitudinal, subsecond dopamine detection in behaving animals. *Nat. Methods* **7**, 126–129 (2010).
- Day, J.J., Roitman, M.F., Wightman, R.M. & Carelli, R.M. Associative learning mediates dynamic shifts in dopamine signaling in the nucleus accumbens. *Nat. Neurosci.* **10**, 1020–1028 (2007).
- Hoffmann, C. *et al.* A FLAsH-based FRET approach to determine G protein-coupled receptor activation in living cells. *Nat. Methods* **2**, 171–176 (2005).
- Falkenburger, B.H., Jensen, J.B. & Hille, B. Kinetics of M1 muscarinic receptor and G protein signaling to phospholipase C in living cells. *J. Gen. Physiol.* **135**, 81–97 (2010).
- Loughlin, S.E. & Fallon, J.H. Substantia nigra and ventral tegmental area projections to cortex: topography and collateralization. *Neuroscience* **11**, 425–435 (1984).

31. Hoover, J.E. & Strick, P.L. The organization of cerebellar and basal ganglia outputs to primary motor cortex as revealed by retrograde transneuronal transport of herpes simplex virus type 1. *J. Neurosci.* **19**, 1446–1463 (1999).
32. Middleton, F.A. & Strick, P.L. Basal-ganglia ‘projections’ to the prefrontal cortex of the primate. *Cereb. Cortex* **12**, 926–935 (2002).
33. Hosp, J.A., Pektanovic, A., Rioult-Pedotti, M.S. & Luft, A.R. Dopaminergic projections from midbrain to primary motor cortex mediate motor skill learning. *J. Neurosci.* **31**, 2481–2487 (2011).
34. Gatter, K.C. & Powell, T.P. The projection of the locus coeruleus upon the neocortex in the macaque monkey. *Neuroscience* **2**, 441–445 (1977).
35. Loughlin, S.E., Foote, S.L. & Bloom, F.E. Efferent projections of nucleus locus coeruleus: topographic organization of cells of origin demonstrated by three-dimensional reconstruction. *Neuroscience* **18**, 291–306 (1986).
36. Zheng, J.Q., Felder, M., Connor, J.A. & Poo, M.-m. Turning of growth cones induced by neurotransmitters. *Nature* **368**, 140–144 (1994).
37. Berg, R.W., Friedman, B., Schroeder, L.F. & Kleinfeld, D. Activation of nucleus basalis facilitates cortical control of a brainstem motor program. *J. Neurophysiol.* **94**, 699–711 (2005).
38. Schulz, K. *et al.* Simultaneous BOLD fMRI and fiber-optic calcium recording in rat neocortex. *Nat. Methods* **9**, 597–602 (2012).
39. Stroh, A. *et al.* Making waves: Initiation and propagation of corticothalamic Ca²⁺ waves *in vivo*. *Neuron* **77**, 1136–1150 (2013).
40. Levene, M.J., Dombeck, D.A., Kasischke, K.A., Molloy, R.P. & Webb, W.W. *In vivo* multiphoton microscopy of deep brain tissue. *J. Neurophysiol.* **91**, 1908–1912 (2004).
41. Jung, J.C., Mehta, A.D., Aksay, E., Stepnoski, R. & Schnitzer, M.J. *In vivo* mammalian brain imaging using one- and two-photon fluorescence microendoscopy. *J. Neurophysiol.* **92**, 3121–3133 (2004).
42. Robinson, D.L. & Wightman, R.M. in *Electrochemical Methods for Neuroscience* Ch. 2, 17–34 (CRC Press, 2007).
43. Okubo, Y. *et al.* Imaging extrasynaptic glutamate dynamics in the brain. *Proc. Natl. Acad. Sci. USA* **107**, 6526–6531 (2010).
44. Marvin, J.S. *et al.* An optimized fluorescent probe for visualizing glutamate neurotransmission. *Nat. Methods* **10**, 162–170 (2013).
45. Romo, R. & Schultz, W. Dopamine neurons of the monkey midbrain: contingencies of responses to active touch during self-initiated arm movements. *J. Neurophysiol.* **63**, 592–606 (1990).
46. Schultz, W., Apicella, P. & Ljungberg, T. Responses of monkey dopamine neurons to reward and conditioned stimuli during successive steps of learning a delayed response task. *J. Neurosci.* **13**, 900–913 (1993).
47. Kosobud, A.E., Harris, G.C. & Chapin, J.K. Behavioral associations of neuronal activity in the ventral tegmental area of the rat. *J. Neurosci.* **14**, 7117–7129 (1994).
48. Miller, J.D., Sanghera, M.K. & German, D.C. Mesencephalic dopaminergic unit activity in the behaviorally conditioned rat. *Life Sci.* **29**, 1255–1263 (1981).
49. Montague, P.R., Dayan, P. & Sejnowski, T.J. A framework for mesencephalic dopamine systems based on predictive Hebbian learning. *J. Neurosci.* **16**, 1936–1947 (1996).
50. Pan, W.X., Schmidt, R., Wickens, J.R. & Hyland, B.I. Dopamine cells respond to predicted events during classical conditioning: evidence for eligibility traces in the reward-learning network. *J. Neurosci.* **25**, 6235–6242 (2005).

ONLINE METHODS

Stably expressing cell lines. To create CNiFERS, we first stably expressed a FRET-based Ca^{2+} -detector, TN-XXL, in HEK293 cells transduced with replication deficient lentivirus as described previously⁵¹. In brief, cDNA for TN-XXL, GPCRs and G_{qi5} as needed was subcloned into the HIV-based cloning plasmid pCDH1-MCS1-EF1-Puro (System Biosciences), and lentiviral particles were produced by the UCSD Vector Development Laboratory (A. Miyanohara, UCSD) or Salk GT³ core. Clonal separation and selection were based on fluorescence intensity using flow cytometry (FACSaria, BD Biosciences) and response to internal calcium concentration increase in the presence of 3 μM ionomycin (Sigma). HEK293 cells were obtained from the ATCC and tested regularly for mycoplasma contamination.

For constructing specific receptor-expressing clones, we used the human D2 receptor (NM_000795; UMR cDNA resource center) and the human α_{1A} (AY389505, UMR cDNA resource center). After selection of a single clone, “TN-XXL only CNiFERS (3g8)” were transduced with lentivirus expressing the α_{1A} adrenergic receptor. For the D2-receptor CNiFER, “TN-XXL only CNiFERS” were first transduced with lentivirus expressing the chimeric G_{qi5} protein to enable coupling of the G_1 -linked D2 receptor with the G_q - Ca^{2+} signaling pathway²³. We identified the best qi5 -expressing clone by transiently expressing the D2 receptor and selecting a qi5 clone that gave the appropriate agonist response with the smallest background response. The qi5 clone was then transduced with a lentivirus that expressed the D2 receptor. Clonal separation and selection was based on fluorescence intensity using flow cytometry. Single α_{1A} CNiFER ($\alpha_{1A.6}$) and D2 CNiFER (D2.2) clones were ultimately selected on the basis of their dose-response curves to both DA and NE (Sigma). All CNiFER cells were maintained at 37 °C with 5% (v/v) CO_2 . Upon confluence, cells were trypsinized, triturated, and seeded into new flasks using Dulbecco’s modification of Eagle’s medium (DMEM) (Cellgro; Mediatech) with 10% (v/v) of Fetalplex serum (Gemini Bio-Products), 100 U/ml of penicillin and 100 $\mu\text{g}/\text{ml}$ of streptavidin (Gibco). Control CNiFERS with only the TN-XXL calcium indicator (3g8) or with TN-XXL calcium indicator and the chimeric G_{qi5} protein (qi5.6) were maintained in the same conditions.

In vitro high-throughput testing. D2- and α_{1A} -CNiFER FRET responses to different neurotransmitters were measured *in vitro* using a high-throughput fluorometric plate reader (FlexStation3, Molecular Devices). The day before the experiments, CNiFERS were plated on fibronectin-coated 96-well plates. Thirty minutes before the experiments, medium in each well was replaced with 100 μl artificial cerebral spinal fluid (ACSF; 125 mM NaCl, 5 mM KCl, 10 mM D-glucose, 10 mM HEPES, 3.1 mM CaCl_2 , 1.3 mM MgCl_2 , pH 7.4), and plates were loaded into the FlexStation3. Experiments were conducted at 37 °C using 436-nm excitation light. Light was collected at 485 ± 10 nm for cyan (ECFP) and 527 ± 12 nm for yellow (Citrine) fluorescent proteins every 3.8 s. After 30 s of baseline, 50 μl of drug diluted in ACSF were delivered to each well. Background measurements taken from wells without cells were subtracted, fluorescence intensities were normalized to prestimulus baselines, and peak responses were measured from the ratio of the 527-nm and 485-nm channels.

In vitro characterization. D2 and α_{1A} CNiFERS were trypsinized and plated on fibronectin-coated coverslips. The following day, CNiFERS were placed in a cell culture chamber (RC26; Warner Instruments) and perfused with gravity-fed ACSF. Chamber fluid temperature was kept at 35 °C by a temperature controller (TC-324B; Warner Instruments). To test the receptor specificity of the D2 CNiFER, we measured FRET responses during two 60-s presentations of 20 nM DA. The second presentation was preceded by 60 s of either 100 nM D1-receptor antagonist, SCH23390 (Tocris), or 50 nM D2-receptor antagonist, eticlopride (Tocris). Percent response remaining was calculated by subtracting the peak FRET response during the second DA presentation (in the presence of antagonist) from the first (in the absence of antagonist). α_{1A} -CNiFER receptor specificity was similarly tested using two 60-s presentations of 50 nM NE, with the second presentation being preceded by 180 s of either 5 μM β -adrenergic-receptor antagonist, sotatol (Tocris), or 50 μM α_{1A} -receptor antagonist, WB4101 (Tocris). For repeat pulse experiments, D2 and α_{1A} CNiFERS were given 10 presentations of 60 s of either 50 nM DA or 500 nM NE, respectively, followed by 180 s of ACSF alone. For temporal discrimination experiments, cells were imaged with a two-photon microscope (see next section), and rapid drug presentation was achieved with a fast perfusion stepper (SF-77B; Warner Instruments). The agonist was mixed with Alexa Fluor 594 in the drug pipette to determine perfusion time. The Alexa 594 signal was imaged simultaneously with the CNiFER FRET response on a third channel.

TPLSM imaging. CNiFER cells were imaged with a custom-built two-photon laser scanning microscope (TPLSM). Control of scanning and data acquisition was achieved through the MPscope software suite⁵². Excitation light at 820 nm was used to excite the ECFP portion of TN-XXL. Fluorescence was collected by either a 25 \times water objective (HCX-IRAPO, Leica) for *in vivo* experiments or a 10 \times air objective (PLAN-NEOFLUAR, Zeiss) for *in vitro* experiments. The fluorescent signal was split into two or three channels: 475 ± 20 nm for measurement of emission by ECFP, 530 ± 20 nm for emission by Citrine and 620 ± 20 nm for emission by Alexa 594.

Animal preparation. Adult, female C57BL/6 mice, age P60–P90, were maintained in standard cages on a natural light-dark cycle. The Institutional Animal Care and Use Committee at the University of California San Diego approved all protocols. For surgery, mice were anesthetized with isoflurane (Butler Schein). Body temperature was monitored and maintained at 37 °C. Subcutaneous injections of 5% (w/v) glucose in saline were given every 2 h for rehydration. Buprenorphine (0.02 mg/kg, Butler Schein) was administered IP for post-operative analgesia.

Retrograde labeling. After anesthesia, mice were placed in a stereotaxic frame. A small craniotomy was performed where CNiFERS were typically injected (+1.5 mm A/P, +1.5 mm M/L). Using a glass pipette with 10- μm inner diameter connected to a Nanoinjector II (Drummond), 200 nl (20 nl every minute) of Fluorogold (Fluorochrome), prepared as 1% (w/v) in 0.1 M cacodylate buffer, was injected in the cortex 200 μm from the surface. After 7 d, the mice were transcardially perfused. Histological sections were scanned at 1- μm spatial resolution using a Nanozoomer

(Hamamatsu) digital slide scanner. Using NeuroLucida software (MicroBrightfield), outlines of midbrain, brainstem and cerebellum were drawn, and sections were aligned based on anatomical borders to yield three-dimensional reconstructions. Outlines of substantia nigra, ventral tegmental area and locus coeruleus were defined by tyrosine hydroxylase-labeled neurons. Cells double-labeled for tyrosine hydroxylase and Fluorogold were marked and counted. Colabeling was confirmed by confocal microscopy.

Histology. Mice were perfused with phosphate buffered saline (PBS), immediately followed by 4% (w/v) paraformaldehyde (PFA) in PBS. Brains were postfixed overnight at 4 °C followed by immersion in 30% (w/v) sucrose. Brain sections, 30- or 50- μm thick, were cut using a sliding microtome. Primary antibodies (mouse anti-tyrosine hydroxylase, 1:1,000, Millipore MAB318, clone LNC1; rabbit anti-Fluorogold, 1:5,000, Millipore AB 153-I; mouse anti-GFAP, 1:1,000, Millipore MAB360, clone GA5; rat anti-MAC1, 1:500, Millipore AB 1387z, clone M1/70.15.1) were diluted in a buffer that consisted of 10% (v/v) goat serum (Vector Labs) and 0.1% (v/v) Triton X-100. Free-floating sections were then incubated overnight under slow rotation at 20 °C in primary antibody solution, washed three times with PBS and incubated with secondary antibody (Alexa 488 anti-mouse, Alexa 594 anti-mouse, Alexa 594 anti-rat and Alexa 594 anti-rabbit, 1:2,000; Molecular Probes A-11001, A-11005, A-11007 and A-11012) for 2 h. Sections were then washed and incubated 15 min in NeuroTrace Blue (Life Technologies), a Nissl stain for visualizing neurons. Sections were washed again and mounted with Fluoromount-G (SouthernBiotech).

CNiFER implantation. CNiFERs were harvested without trypsin from 80% confluent culture flasks, centrifuged and resuspended in ACSF for injection. For the *in vivo* dose-response experiment, an open craniotomy was used. For all other *in vivo* experiments, a 'thinned skull' craniotomy¹⁷ was used. CNiFER cells were loaded into a 40- μm -inner diameter glass pipette connected to a Nanoinjector II (Drummond) and injected into neocortex through the thinned skull $\sim 200\ \mu\text{m}$ from the cortical surface. CNiFERs were injected into adjacent sites within the following stereotaxic coordinates: +1 to +2 mm A/P; +1 to +2 mm M/L. After implantation in several adjacent sites (typically two injection sites per CNiFER variant), the craniotomy was sealed with a glass coverslip. A custom-built head-bar was attached to the skull with C&B-Metabond (Parkell), and the preparation surrounding the imaging window was covered with dental cement (Dentsply). Mice were immunosuppressed by daily cyclosporine injection (20 μl per 100 g, IP, Belford Laboratories).

Electrical stimulation and *in vivo* pharmacology. Mice were prepared and injected with CNiFERs as described. Additionally, a 0.1-M Ω tungsten bipolar stimulating electrode with a tip separation of 500 μm (MicroProbes) was implanted into either the substantia nigra (-3.2 mm A/P, -1.3 mm M/L, -4.4 mm D/V) or the locus coeruleus (-5.3 mm A/P, -0.9 mm M/L, -3.4 mm D/V). After a day of recovery, imaging was performed under isoflurane anesthesia. Experimental runs consisted of a 30-s baseline followed by electrical stimulation (200- μs pulses of 50–300 μA at 50 Hz for 500 ms). To test the specificity of the response, we IP-injected eticlopride (1 mg/kg, Sigma),

WB4101 (2 mg/kg, Tocris), or cocaine (15 mg/kg; Sigma) 10 min before the electrical stimulation.

***In vivo* dose response.** After CNiFER implantation, the craniotomy was kept open and a glass pipette connected to a Nanoinjector II (Drummond) was positioned, using a Sutter manipulator, 100 μm away from the CNiFER implants. Imaging was performed under urethane anesthesia (1.5 g/kg, IP). The agonist, i.e., NE or DA, was mixed with Alexa 594 to verify the arrival of the agonist as well as to calculate the dilution of the agonist between the pipette and the implant. A long train of pulses of agonist (2.3-nl pressure injections as 2-s pulses every 5 s until a steady-state response was observed, typically after 30 s) was then applied next to the CNiFER implants. Control pulses of Alexa 594 in saline did not cause any FRET change. The dilution was calculated by measuring the average fluorescence of Alexa 594 in the interstitial space of the implant and comparing it to the average fluorescence of the dye in the void immediately downstream from the pipette.

***In vivo* awake imaging and behavior.** After 1 d of recovery from surgery, mice were water deprived (23 h per day). Conditioning started the following day. Animals were placed in a stationary head-frame and imaged while being presented with a 5-s tone (CS) followed by a 3-s delay and a drop of 10% (w/v) sucrose water (US), with an average intertrial interval of 3 min. Two CNiFER variants, i.e., the α_{1A} and D2 CNiFERs or the M1 and D2 CNiFERs, were imaged simultaneously. Licking behavior was recorded using a custom-built, conductance-based sensor. Mice were imaged for 10–15 trials and then returned to their home cage. Animals were imaged once a day for 5 consecutive days.

Data analysis. All the TPLSM data analysis was done using Matlab (MathWorks). TN-XXL fluorescence intensities were background subtracted and normalized to prestimulus baselines. Regions of interest were drawn around either the D2- or the α_{1A} -CNiFER implants. Responses were quantified as the fractional change in the FRET ratio $\Delta R/R$, where ΔR is the change in the ratio of fluorescence intensities of the two channels, denoted $F_{530\text{nm}}$ and $F_{475\text{nm}}$, respectively, and R is the normalized baseline ratio, such that

$$\frac{\Delta R(t)}{R} = \left(\frac{F_{530\text{nm}}(t) / \langle F_{530\text{nm}}^{\text{baseline}} \rangle_{\text{prestim}}}{F_{475\text{nm}}(t) / \langle F_{475\text{nm}}^{\text{baseline}} \rangle_{\text{prestim}}} \right) - 1$$

Responses were measured at the peak of $\Delta R/R$ after low-pass filtering. For *in vitro* high-throughput testing, the peak responses were determined using Matlab, and the EC₅₀ and Hill coefficient were calculated using Prism software (GraphPad). For behavioral experiments, the onset of the FRET signal was analyzed using Matlab. The onset of the FRET signal was defined as the point at which the ratio $\Delta R/R$ increased by 2.5 times the r.m.s. level of the baseline noise, typically $\Delta R/R \approx 0.03$. Each onset time was scored manually by two experimenters that were blind to the time of the CS and the US. Only trials in which animals responded after CS presentation and within 30 s of US presentation were used for analysis. We excluded animals for which the imaging windows did not allow us to observe the entire experiment (through day 5 of conditioning), a preestablished criterion. No randomization was used. Statistical analyses were calculated using Prism software (GraphPad).

For linear regressions, we used a cutoff of $P \leq 0.05$ to determine whether the slope was significantly different from 0. When analyzing FRET onset times over time, we confirmed the difference between day 1, day 3 and day 5 with a one-way ANOVA test.

51. Mank, M. *et al.* A genetically encoded calcium indicator for chronic *in vivo* two-photon imaging. *Nat. Methods* **5**, 805–811 (2008).
52. Nguyen, Q.-T., Driscoll, J., Dolnick, E.M. & Kleinfeld, D. in *In Vivo. Optical Imaging of Brain Function* 2nd edn. (ed. Frostig, R.D.) Ch. 4, 117–142 (CRC Press, 2009).